Influence of the Photosystem I−Light Harvesting Complex I Antenna Domains on Fluorescence Decay

Enrico Engelmann, Giuseppe Zucchelli, Anna Paola Casazza, Doriano Brogioli, Flavio M. Garlaschi, and Robert C. Jennings*

Istituto di Biofisica del Consiglio Nazionale delle Ricerche−Sezione di Milano, Dipartimento di Biologia, Università degli Studi di Milano, via Celoria, 26, 20133 Milano, Italy

Received February 6, 2006; Revised Manuscript Received March 22, 2006

ABSTRACT: The time-resolved fluorescence decay of plant PSI−LHCI has been analyzed and compared with its component parts, the PSI core and the peripheral antenna LHCI, in an attempt to (i) define the physical domains associated with the multicomponent decay-associated spectra (DAS) and determine the origin of the kinetically slow steps responsible for them, (ii) formulate a clear working hypothesis for the positive decay-associated spectral amplitudes of the two slowest decay components, and (iii) determine the impact of the peripheral antenna complexes (LHCI) on the effective trapping rate for the photosystem. The results for PSI−LHCI indicate that the three exponential component DAS description, previously reported in the literature, is not numerically unique. The fit minimum is rather broad, which necessitated the introduction of other fit criteria in addition to the purely numerical one. The analysis demonstrates that (i) the physical domains associated with the multicomponent decay are associated with the antenna and particularly with the low-energy spectral forms, (ii) the positive DAS amplitudes of the two slowest decay components are suggested to be due to energy transfer kinetic heterogeneity to different F735 low-energy forms, and (iii) the peripheral antenna slows down the effective photosystem photochemical rate by about 3 times, and this is approximately half due to antenna degeneracy and half due to the low-energy forms.

Photosystem I (PSI)[1] of higher plants is a supramolecular pigment/protein complex, localized in the nonappressed regions of thylakoid membranes. The complex binds the primary electron donor chlorophylls (chls), known as P700, and can photoreduce ferredoxin using plastocyanin and cytochromes as secondary electron donors (*1*). The complex has two moieties, which are the central chl *a*-binding core complex and a peripheral antenna which consists of four chlorophyll *a*/*b* binding proteins known collectively as LHCI. The core complex binds approximately 95 chl *a* and probably about 20 carotene molecules (*2*−*4*) as well as P700 and the primary acceptors A0 and A1 at the interface between the two homologous subunits (*2*). The LHCI complexes seem to be arranged on one side of the core (*2*, *5*), and taken together, they bind about 66 chl *a* + *b* according to the crystallographic structure (*2*) and 80−100 according to biochemical analysis (*6*), and 20 xanthophylls, with the number of complexes surrounding the core probably being four according to the crystallographic structure and around 10 according to biochemical analysis (*6*). The LHCI complexes are now known to bind around 15−16 chlorophylls per monomer (*2*). The PSI−LHCI complex can be isolated in an intact form, that is, without detergent-solubilized chls present (*7*). In the region of the lowest lying electronic transition (Q_y), the complex has a broad absorption band with its maximum at 680 nm. This band is associated with the so-called ''bulk" antenna chl *a* and accounts for about 90−95% of the Q_y oscillator strength. Owing to the broadness of this band, the approximately 15−20 chl *b* molecules cannot be resolved from the 150−155 chl *a* molecules in absorption spectra, even at cryogenic temperatures. However, it is known that their Q_y transition is near 650 nm from analysis of the isolated LHCI complexes (*8*). A peculiarity of the PSI−LHCI absorption spectrum is the presence of significant absorption in the low-energy tail, indicating the presence of red spectral chl *a* forms, or states, absorbing at energies lower than that of the primary donor P700. Their combined oscillator strength is approximately equivalent to 7−8 chls (*7*) which in the steady state are highly populated, with 80−90% of the PSI−LHCI excited states being associated with them (*7*). It has now been experimentally demonstrated that the red forms, located in the peripheral antenna in plant PSI−LHCI, are kinetically limiting for the transfer of energy from the antenna to the reaction center (*9*−*11*), though the exact extent of this slowing down has not been clearly established to date.

From the above brief description of plant PSI it is clear that its antenna system is quite complicated, in particular, by virtue of the presence of the low-energy chlorophyll forms in the peripheral antenna. In this context it is interesting to note that the several fluorescence lifetime studies which have been performed on PSI−LHCI indicate a multiexponential

* Corresponding author. E-mail: Robert.jennings@unimi.it. Fax: +390250314815. Phone: +390250314858.

[1] Abbreviations: chl, chlorophyll; DAS, decay-associated spectrum; Lhca1−4, subunits of the light harvesting complex I; LHCI, light harvesting complex I; LHCII, light harvesting complex II; PSI, photosystem I; Fwhm, full width at half-maximum.

10.1021/bi060243p CCC: $33.50
Published on Web 05/03/2006

decay (*9*, *12*, *13*). At room temperature, and with an approximately 10 ps time resolution, two and perhaps three trapping-associated decays are apparent, and at 170 K an extra trapping-associated decay component becomes detectable (*9*). An important question concerning plant PSI function is the origin of these decay components. In general, two possibilities may be distinguished to account for multiple decays in PSI: (i) they may be brought about by slow antenna energy transfer processes associated with the red forms of LHCI, or (ii) they could be due to reversible charge separation reactions. In the recent literature evidence exists for both of these mechanisms. Involvement of the red forms is suggested by the demonstration that energy equilibration with these low-energy states is slow (*9*), i.e., on the same time scale as the fluorescence decay itself. In addition, the trapping-associated decay from these red forms is slower than from the "bulk chlorophylls" (*10*), indicating that they exert a kinetic limitation on the overall photosystem effective trapping rate. The thermal "activation" energy for trapping was found to be in the range 3−5 kT at room temperature, consistent with a rate-limiting effect. On the other hand, Holzwarth and co-workers, working with the alga *Chlamydomonas reinhardtii* (*14*, *15*), provide extensive ultrafast kinetic, model-based evidence for a reversible charge separation within the PSI reaction center. Central to this interpretation is a major overall core trapping component of about 8 ps, associated with the suggestion that the reaction center/antenna equilibration time is about 1 ps. These suggested rate processes are much faster than those suggested in extensive previous work by a number of laboratories on core complexes from cyanobacteria (e.g., refs *16* and *17*). Whether or not this suggestion is applicable to plant PSI is open to conjecture; however, it is usually believed that reaction center characteristics are well conserved in different groups of organisms.

Another aspect of basic interest is the overall effect of the outer antenna on the effective photochemical charge separation rate at the level of the photosystem. We have recently examined this aspect for photosystem II where it was shown that the outer, or peripheral, antenna slows down the photosystem effective trapping rate $(\tau_{cs}^{eff})^{-1}$ by an approximately 2.5-fold factor (*18*), i.e., from around $(170\ ps)^{-1}$ for the core to approximately $(450\ ps)^{-1}$ for the core *plus* outer antenna. This factor was somewhat less than expected on the basis of simple model considerations. In the case of PSI similar studies are lacking and are expected to be interesting in that the two photosystems have very different antenna characteristics. First, PSII is composed of almost isoenergetic antenna (domain) complexes (*19*, *20*) whereas in PSI the outer antenna (LHCI) complexes contain low-energy chlorophylls. Second, for PSII, the outer antenna/core antenna chl *a* ratio is about 3.3 while in PSI it is close to 0.7.

With these aspects in mind we have performed fluorescence lifetime measurements on maize PSI−LHCI and its component parts, the PSI core, and LHCI. While fluorescence lifetime studies of similar preparations of both PSI−LHCI and LHCI have already been analyzed in the literature (*9*, *17*), the PSI core from plants has not. In addition, the earlier study on maize PSI−LHCI was performed in the presence of high concentrations of glycerol which we show here slow down τ_{cs}^{eff}. It should also be mentioned that unavoidable kinetic differences are observed from preparation to preparation and also measurement differences may occur from instrument to instrument. In the present work we have attempted to minimize these problems by making all preparations from the same starting material, and obviously the same instrument was used for all measurements.

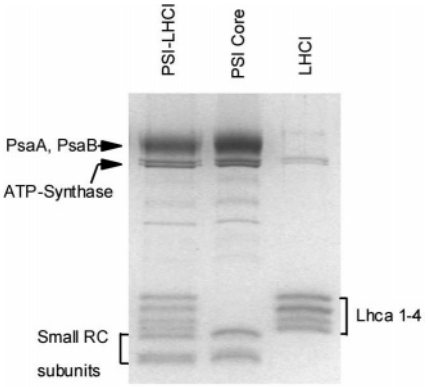

FIGURE 1: SDS−PAGE polypeptide composition of PSI−LHCI and the core and LHCI preparations which derived from it. The gel band identifications are on the figure.

MATERIALS AND METHODS

PSI−LHCI, PSI core, and LHCI were purified from PSI−LHCI as previously described (*7*, *8*). The samples were characterized on the basis of their Q_y absorption spectra and polypeptide composition. The absorption spectra were similar to those previously reported (*8*) (data not presented). Polypeptide composition was confirmed by SDS−PAGE (Figure 1) using 15% polyacrylamide gels in 6 M urea (*21*) (Laemmli discontinuous buffer system). Samples, equivalent to 1.3 μg of chlorophyll, were loaded in the wells.

Time-esolved (picosecond) fluorescence decay measurements of PSI−LHCI and the PSI core were performed in a 10 mM Tricine buffer in the presence of an oxygen scavenger system (glucose/glucose oxidase/catalase) and the redox mediator phenazine methosulfate (PMS, 20 μM)/sodium ascorbate (220 μM) using the time-correlated single photon counting technique (TCSPC) with excitation at 632 nm. The excitation source was a pulsed diode laser (PicoQuant GmbH, Berlin Germany), peaked at 632 nm, controlled by a controller, PicoQuant PDL 800-B, and operating at a repetition rate 40 MHz. We estimate that under these conditions the sample absorption flux is approximately 0.4×10^{15} photons s^{-1}, which gives a mean value of 0.03 photon ms^{-1} for each PSI−LHCI complex. For the PSI core the absorption flux was about 0.015 photon ms^{-1} for each complex and for the LHCI complexes 0.002 photon ms^{-1} for each complex. Thus triplet accumulation is not expected. In addition, it is known that the triplet yield of PSI antenna pigments is extremely low (*22*, *23*). The emission decays were passed through a monochromator (Jasco CT-10) and detected by a microchannel plate photomultiplier tube (Hamamatsu R3809U-51). Samples were changed every hour. The instrumental response function (IRF) was measured as the profile of the intensity of light scattered by a turbid, nonfluorescent sample, measured at the excitation wavelength; its fwhm was 80 ps. The measured fluorescence decay is modeled as the convolution of the IRF with a sum of exponentials; the resulting curve is fitted to the experimental

data by minimizing the χ^2. Fit parameters are the time decay constants, the decay amplitudes, the offset of the time scale, and the background (dark) intensity. The minimization has been performed by means of an algorithm developed in the laboratory, based on the Minuit library from CERN, distributed with a c-fortran interface as "c-minuit". Both the c-minuit and our Minuit-based algorithm are freely available as open-source software [https://sourceforge.net/projects/multiexpfit; https://sourceforge.net/projects/c-minuit]. The algorithm allows not only the minimization but also error analysis and determination of χ^2 hyperspace sections. The emission decays were usually recorded at 10 nm intervals between 680 and 770 nm; the analysis was performed globally.

RESULTS AND DISCUSSION

Previous fluorescence decay studies on PSI−LHCI describe the room temperature decay in terms of essentially three components. The fastest, which has been reported to have lifetimes in the range 5−11 ps, has both positive and negative amplitudes and therefore possesses antenna excited state transfer characteristics. The other two decays have only positive amplitudes and have been reported in the lifetime range 20−60 and 80−130 ps, respectively (*9*, *12*, *13*, *24*). It is also usually found that the positive amplitude components become red shifted with increasing lifetime, an aspect which has been discussed in terms of the thermal activation energy of trapping from the spectral forms (*10*). We have therefore sought descriptions with this type of characteristic, and Figure 2A shows a typical three-component decay of PSI−LHCI, of this kind, in terms of the decay-associated spectra (DAS). There are, however, analytical uncertainties associated with this description which we discuss below.

Owing to the rather broad spread of decay times in the literature we have investigated the χ^2 parameter hyperspace, which was found to be broad and "rough" for the single measurements analyzed globally. We therefore performed a number (five) of separate measurements which were subjected to a simultaneous global analysis. The reduced χ^2 parameter hyperspace lost the above-described rough character, though it remained rather broad. The absolute numerical minimum of this simultaneous global analysis yielded lifetimes of approximately 10, 60, and 124 ps in which the 10 ps decay, of dominating amplitude, did not possess the usually observed energy transfer characteristics; i.e., only positive amplitudes were present. This numerical minimum description also displayed DAS band shape variability between separate measurements. In addition, we noticed that the solution was very sensitive to the temporal shift between the instrumental response function (δ) and the measured fluorescence decays. In fluorescence decay measurements this parameter is not known and is considered as a fit parameter. Changing by just 5 ps, a value below our instrumental response time, caused the switching between a description with a transfer component present to a solution where no transfer component was present. The DAS of the other two decay components shown were less influenced by the temporal shift. For these reasons we interpret the absolute numerical minimum as providing a not completely satisfactory description and decided therefore to adopt as additional fit criteria that the DAS description should display stability for the DAS band shapes between measurements and that

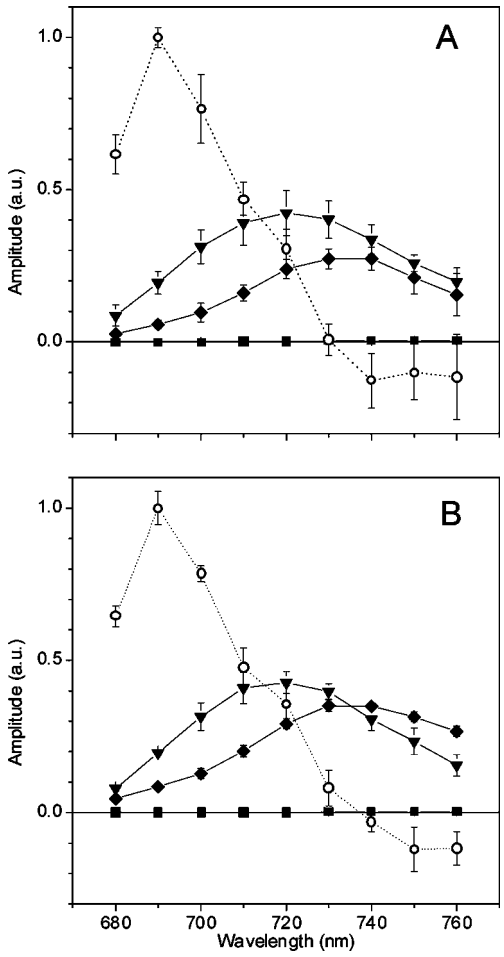

FIGURE 2: (A) Decay-associated spectra (DAS) of the PSI−LHCI preparation measured at 280 K: circles, 11 ± 2 ps; triangles, 30 ± 3 ps; diamonds, 79 ± 5 ps; squares, 0.8 ns. Each point represents the average of five separate measurements, and the error bars are the standard deviations. (B) Decay-associated spectra (DAS) of the PSI−LHCI preparation incubated in glycerol (65% v/v) and measured at 280 K: circles, 11 ± 1 ps; triangles, 33 ±2 ps; diamonds, 93 ± 5 ps; squares, 1.01 ns. The data have been obtained from four separate measurements, and the error bars are the standard deviations.

the usually observed transfer component should be present. This was achieved by searching for such a description within the broad minimum hyperspace. A good example of such a description is shown in Figure 2A.

The solution presented in Figure 2A, with its associated intersample errors, can thus be regarded as an approximation for the DAS decay times and amplitudes, which may in fact display an even greater distribution than our intersample errors indicate. We are therefore of the opinion that it is probably not appropriate to attempt to search for an exact model description based on these parameters.

In this description (Figure 2A) the fastest component detectable has an apparent decay time of 11 ± 2 ps, as previously described (*9*). We emphasize that our instrument resolution is approximately 10 ps. This decay has both positive and negative amplitudes, which indicate that it represents, at least in part, excitation flow from the bulk antenna to the red forms. Ihalainen et al. (*13*), with a streak camera resolution of 1−3 ps and working with *Arabidopsis* PSI−LHCI prepared in the same way, detected an approximately 5 ps pure transfer component. As we are

primarily interested in reaction center trapping, such unresolved fast transfer components are not of relevance to this analysis. The 11 ps DAS is distinctly nonconservative, as previously observed (*9*, *13*), which may indicate a small fraction of excited states which are rapidly trapped. From the relation $\sum A_i(\lambda)\tau_i/(\sum A_i(\lambda)\tau_i + \sum A_j(\lambda)\tau_j + \sum A_k(\lambda)\tau_k)$ we estimate that the fraction of fast decaying excited states has a maximal value of about 10% of the total excited state population for the wavelength interval 670−750 nm, where *i*, *j*, and *k* represent the three decays (11, 30, and 79 ps). However, given the above-mentioned uncertainties associated with the temporal shift (δ), one must be careful in not overinterpreting this. The 30 ± 3 and 79 ± 5 ps decay components have DAS maxima near 720 and 730−740 nm, respectively, as previously described for the maize PSI−LHCI. However, it will be noticed that the present decays are faster than the 57 and 130 ps decays previously reported for the maize PSI−LHCI preparation (*9*), and the slowest decay has a lower relative DAS amplitude at all wavelengths to that described in the earlier study. The value for the mean lifetime of the total fluorescence decay in the wavelength interval 690−780 nm ($\tau_m = \sum A_i(\lambda)\tau_i^2/\sum A_i(\lambda)\tau_i$) reported by Croce et al. (*9*) was 99 ps, whereas in the present case this value is 60 ps for a similar wavelength interval (680−770 nm). To examine this situation, we initially checked our instrument resolution using the DCI′ dye (1,1′-diethyl-2,4′-carbocyanine iodide), having an excited state lifetime of 20 ps, in an ethanol solution (Laser Dyes Catalogue, Exciton, Inc., P.O. Box 31126, Dayton, OH; www.exciton.com). This lifetime was accurately retrieved using our setup (data not shown), indicating that our resolution is presumably good also for somewhat shorter lifetimes.

As the previous measurements of Croce et al. (*9*) were performed at cryogenic temperatures, as well as room temperature, the cryoprotectant glycerol was present in the reaction mixture. We have therefore examined the effect of glycerol on the fluorescence decay of PSI−LHCI, and the DAS are presented in Figure 2B. The initial multiexponential decomposition used the same initial search conditions as those for Figure 2A. It is evident that glycerol does in fact influence the fluorescence decay, primarily by increasing both the component decay time from 79 ± 5 to 93 ± 5 ps and the relative amplitude of the slowest DAS component. The relative amplitudes of the 30/80ps DAS are now very similar to those presented earlier (*9*), and the crossover wavelength of the two slowest components is near 740 nm in the presence of glycerol, as in the earlier study (*9*). The value of τ_m increases from 60 ps in the absence of glycerol to 80 ps in its presence. It is interesting to note that the DAS band shapes are apparently unchanged by glycerol incubation (Figure 2), which suggests that its slowing down effect may not be on antenna processes. These data therefore indicate that the effective photosystem trapping time for PSI−LHCI is probably somewhat faster than was previously suggested. These results have been confirmed using three different PSI−LHCI preparations.

In the following we will discuss the two slowest decay components in the non-glycerol samples (30 ± 3 and 79 ± 5 ps). As mentioned above, these account for the trapping of 90% of excited states in the PSI−LHCI sample, and as previously reported, both have only positive amplitude values, which for a coupled system of first-order rate processes is unexpected. From a mathematical point of view only the slowest decay should be "all positive". This interesting point was specifically addressed some time ago by Trinkunas and Holzwarth (*25*, *26*). In principle, this may suggest that the explanation be sought in terms of reversible relaxation processes occurring during primary charge separation, as recently suggested by Holzwarth and colleagues (*14*, *15*) for *Chlamydomonas* PSI. In this case the negative amplitude processes are expected to occur within the reaction center and would then not be detected in these fluorescence measurements. To study this point, we have purified the PSI core from the same batch of PSI−LHCI and analyzed its fluorescence decay. If reversible charge separation processes occurring in the reaction center do in fact generate the ≈30 and ≈79 ps decay components detected in PSI−LHCI, a clear multicomponent decay should also be detectable in the PSI core, particularly as the core antenna seems to be well over 50% that of PSI−LHCI (*2*). Data for the core fluorescence decay are presented in Figure 3, where almost all of the DAS amplitude is associated with a 17 ± 5 ps decay. It is evident that this component represents the core decay. The small amplitude DAS with a 70 ± 15 ps decay time is thought to be a minor contamination, with unfractionated PSI−LHCI, which is of the order of 2% on the basis of the relative amplitudes. A small amount of uncoupled LHCI is also detected with a nanosecond lifetime. It should be noted that the 17 ± 5 ps decay possesses a weak shoulder at 720−730 nm, indicating a low presence of long-wavelength amplitudes. Their content, however, is considerably lower than that encountered in the PSI−LHCI (Figure 2) and also lower than that detected in our earlier study on the PSI core from plants by means of steady-state fluorescence measurements (*8*). This discrepancy may be due to somewhat higher levels of contamination by the PSI−LHCI decay in the earlier preparation. The weakness of the long-wavelength signal in the 17 ps DAS underlines our earlier conclusion that most red forms are associated with LHCI in plant PSI−LHCI (*8*). Thus the maize PSI core has an essentially monoexponential fluorescence decay with the present experimental resolution of about 10 ps. While this conclusion is essentially in agreement with the model studies

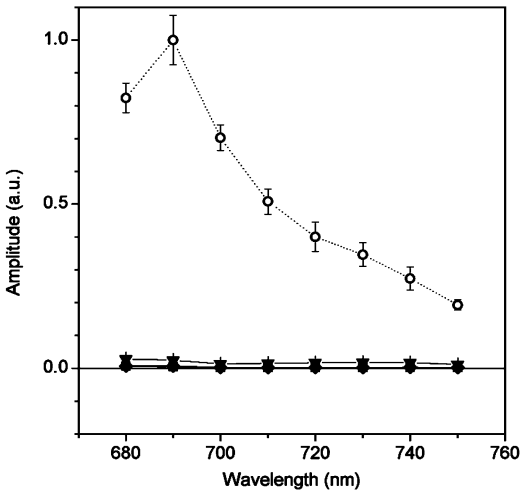

FIGURE 3: Decay-associated spectra of the PSI core preparation measured at 280 K: circles, 17 ± 5 ps; stars, 70 ± 15 ps; dots, 1 ns. Data are from 10 separate measurements, and the error bars are the standard deviations.

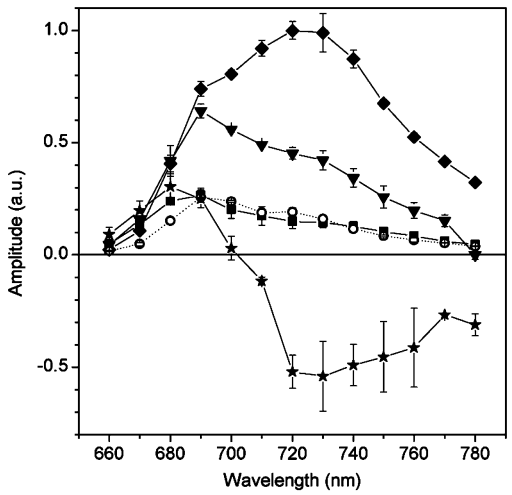

FIGURE 4: Decay-associated spectra of the maize LHCI preparation: stars, 20 ± 5 ps; open dots, 125 ± 13 ps; triangles, 1.45 ± 0.2 ns; diamonds, 2.7 ± 0.1 ns; squares, 3.8 ± 0.2 ns. Data are from four separate experiments, and the error bars are the standard deviations.

of the PSI cyanobacterial core (*17*, *25*), the presence of a faster trapping component cannot be entirely excluded, particularly as Holzwarth et al. (*15*) has recently suggested that an 8 ps trapping decay is present in the *Chlamydomonas* core. On the other hand, previous studies did not detect this component. Hastings et al. (*16*) and Gobets et al. (*17*), analyzing a variety of cyanobacterial PSI core particles, with streak camera resolution of 1−3 ps, did in fact discern a 3−4 ps component. However, in all cases, this was described as a pure transfer component with no reaction center trapping evident. As the 8 ps trapping decay suggested by Holzwarth et al. (*15*) is only slightly below our instrumental resolution, we expect that it should be detectable also in our measurements, albeit not well resolved. To examine this more closely, we modified the starting conditions for the fluorescence global decay decomposition by adding an additional exponential of 10 ps, which was not in any way fixed. This decay subsequently was found to "move" toward the 17 ps decay and had an almost identical DAS band shape. We are therefore forced to conclude that the 8 ps trapping component, suggested to be present in the *Chlamydomonas* core, seems not to be present in the plant PSI core. We therefore conclude that the plant PSI core does not display the biexponential trapping decay evident in the PSI−LHCI. This conclusion favors an outer antenna (LHCI) origin for these components in PSI−LHCI and thus suggests that a slow, kinetically rate limiting, transfer process occurs in the outer antenna which generates the 30 and 80 ps components in PSI−LHCI.

We have also purified the LHCI fraction from the parent PSI−LHCI preparation and analyzed its fluorescence decay. An adequate description requires a minimum of five exponential components, and the DAS description of Figure 4 is, in general terms, comparable to that previously published for a similar LHCI preparation by Ihalainen et al. (*27*). The fastest decay (20 ± 5 ps) represents transfer from the bulk chlorophylls to the red forms. It will be noticed that this transfer time (20 ± 5 ps) is apparently slower than the equivalent decay in PSI−LHCI (11 ± 2 ps). This is readily explained by the absence of photochemical trapping in LHCI, as this process, in physical terms, competes with the antenna

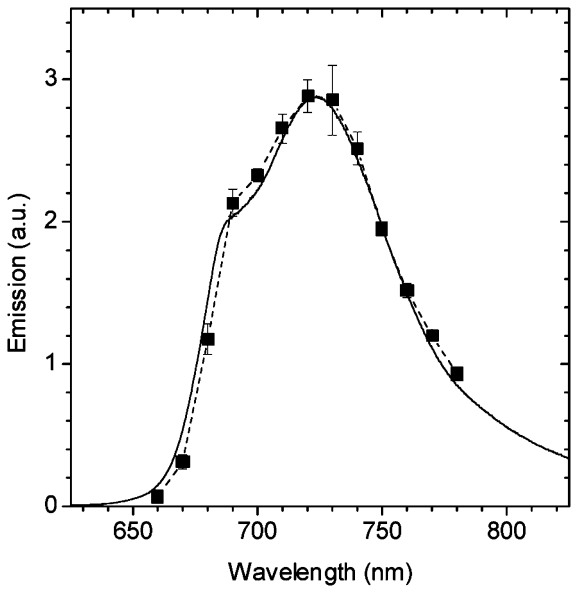

FIGURE 5: Fluorescence band shapes of (i) the steady-state emission of Lhca4, nonselectively excited (continuous line), and (ii) the ≈2.75 ns decay-associated spectrum of native LHCI (squares). The Lhca4 spectrum is taken from Zucchelli et al. (*30*).

transfer process for antenna excitons. Thus when it is removed, as in the isolated antenna complexes, the antenna transfer process is somewhat slower. It can be shown, by the compartmental model of Figure 8B, that this slowing down is expected to be of an approximately 2-fold factor, just as we observe. The other four components have only positive amplitudes and to a large extent, probably, represent the decay of the four Lhca1−4 complexes present in this preparation. The two long lifetime decays (3.8 ± 0.2 and 2.7 ± 0.1 ns), with pronounced long-wavelength DAS amplitudes, are probably the origin of the red-shifted ≈30 and ≈79 ps components of PSI−LHCI (Figure 2). The 2.7 ns component most likely represents the Lhca 4 monomer, as this complex has been shown to contain the highest content of red forms (*28*) which emit at both 735 and 713 nm (*29*). In agreement with this interpretation is the close correspondence in band shape between the recombinant Lhca 4 [data from Zucchelli et al. (*30*)] and the DAS for the 2.7 ns decay (Figure 5).

We now address the question of the origin of the ≈30 and ≈79 ps DAS in PSI−LHCI. As is evident from Figure 2 the 79 ps component is red shifted with respect to the 30 ps one. This has already been observed for the maize PSI−LHCI preparation (*9*, *10*). In their study on *Arabidopsis* PSI−LHCI, Ihalainen et al. (*13*) suggested that the faster decay might originate in the core antenna, and in a very recent publication by the same group (*24*) this point was underlined again. It should be noted, however, that the DAS lifetimes and band shapes for the *Arabidopsis* PSI presented in these two papers are rather different, probably due to the broad global fit minimum discussed above in this paper. As this point is not discussed by Ihalainen et al. (*13*, *24*), we are unable to evaluate this aspect. We would also point out that if the PSI core is well coupled energetically to the LHCI complexes, as is expected, there should *not* be a separate core-based decay. It is expected to be mixed in with the other antenna components (LHCI). In this context we note that the DAS band shapes of the ≈30 ps component (Figure 2)

indicate a high red-form content, which we conclude above as being associated with a substantial contribution from the long lifetime LHCI decays. On the contrary, the isolated core (Figure 3) has a low red-form content. These data are not in agreement with the suggestion of Ihalainen et al. (*13*, *24*). Both the ≈30 and ≈79 ps DAS band shapes are dominated by the low-energy emitting forms of the outer antenna (LHCI).

In a recent series of studies it has been demonstrated that isolated LHCI and recombinant Lhca 4 possess at least two distinct red forms, F735 and F713 (*10*, *29*, *30*). The emission band shape of F735 was directly measured at room temperature, and that of F713 was subsequently deduced by analysis of difference spectra. The fluorescence bandwidth of F735 is approximately 50 nm at room temperature while that of F713 is approximately 27 nm. In the following we compare the DAS band shapes for the long-wavelength emitting interval ($\lambda \geq 710$ nm) with these two LHCI emitting forms. We are addressing the question as to whether the band shapes of these two low-energy species are able to reasonably describe these two DAS band shapes in the red-most region. We do not attempt to analyze the 670−700 nm interval in this way as the spectral normalization procedure used to determine the F735 and F713 band shapes was based on the emission shoulder of the bulk emission near 685 nm. This may have led to an apparent narrowing of the band shapes below about 700 nm and hence some underestimation of their DAS contribution in this wavelength interval. We therefore consider this comparison of the DAS with the F735 and F713 band shapes to be reliable only above 700 nm.

The data for both the ≈30 and the ≈79 ps decay are shown in Figure 6. In Figure 6A the ≈79 ps DAS, which is the most red shifted of the two, is overlaid with the F735 band shape. The two spectra overlap well in the wavelength range 740−770 nm, with the 79 ps DAS displaying greater intensity (amplitude) at 710−730 nm. This leads to the conclusion that the slowest PSI decay seems to be mainly associated with the lowest energy form F735 with a possible small contribution by F713. By manipulation of the F735 nm and the F713 band shape contributions, it can be shown (Figure 6B) that the ≈79 ps DAS is well described by these two bands with relative weightings of approximately 0.9 (F735) and 0.1 (F713). We have not attempted to describe the DAS amplitudes at 700 nm and below, where bulk emission is undoubtedly present, due to our above-mentioned reservations concerning the F735 and F713 band shapes in this region. In addition, we point out that we have not attempted to include the long-wavelength emission, apparently present in the core, in this description. This is because of its low intensity in the core which would be further "diluted out" in PSI−LHCI. It is interesting to note that the two red forms originating in LHCI are sufficient to obtain a good description of the two DAS band shapes in the long-wavelength region.

We now discuss the broad and rather symmetrical 30 ps DAS which peaks in around 720 nm. Owing to the above-mentioned bandwidths of the F713 and F735 it is expected that the red-most region of the 30 ps decay is associated exclusively with F735. This expectation is borne out in Figure 6B where the two spectra overlap well above 740 nm where F713 emission is close to zero. Below this wavelength other antenna contributions, from both the F713 and bulk antenna, are present. This DAS can be quite accurately described in the 710−760 nm interval by using just the F735 and F713 band shapes with relative weightings of approximately 0.7 and 0.3, respectively (Figure 6B).

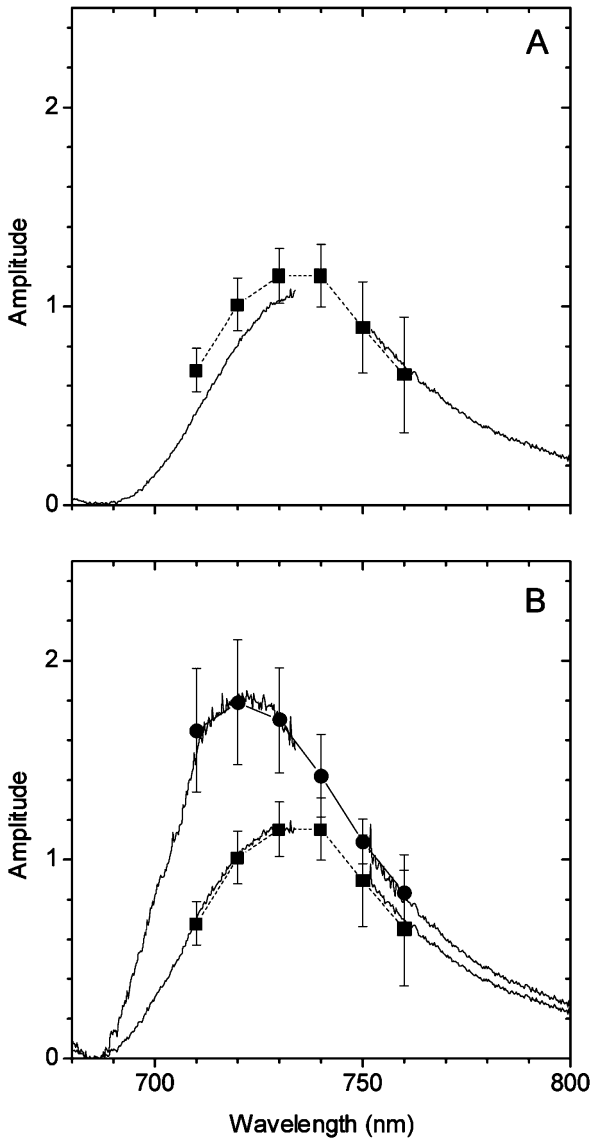

FIGURE 6: (A) The ≈79 ps DAS band shape of PSI−LHCI between 710 and 760 nm (squares) overlaid with the F735 spectral form band shape (continuous line). (B) The ≈79 and ≈30 ps DAS band shapes between 710 and 760 nm and the respective fits with F735 (0.9) and F713 (0.1) for the ≈79 ps DAS (lower curve) and F735 (0.7) and F713 (0.3) for the ≈30 ps DAS (upper curve). The respective fit weighting factors are indicated in parentheses and refer to the areas subtended by F735 and F713 in the fit.

These observations demonstrate that, within the present experimental uncertainty, it is possible to describe both the ≈30 and ≈79 ps decays of PSI−LHCI, in the long-wavelength region, by different combinations of F735 and F713, the two emitting forms present in LHCI. This is the first time such a clear description of the PSI−LHCI fluorescence DAS band shapes has been presented. It furthermore suggests that the presence of these two decay components is generated by slow antenna processes. If they were due to reversible reaction center processes, after rapid antenna/reaction center equilibration, it is difficult to envisage such large differences in the DAS band shapes due to antenna

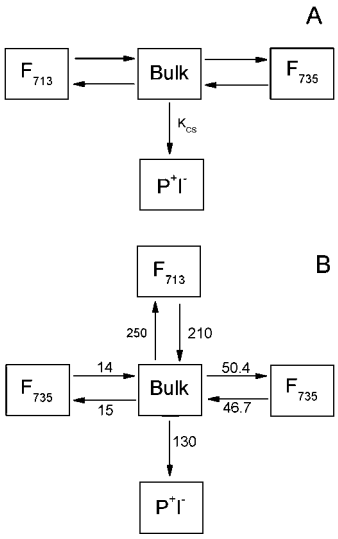

FIGURE 7: Compartmental models for the decay-associated spectra which describe the fluorescence decay of PSI−LHCI: (A) minimal model; (B) model in which two populations of F735 are included, for which the energy transfer rate to and from the bulk is heterogeneous. The numbers above the arrows are an example of the rate constants (in ns^{-1}) which satisfactorily describe the DAS presented in Figure 2A. Owing to the broadness of the fit minimum (see text) these rates should be viewed as being purely indicative.

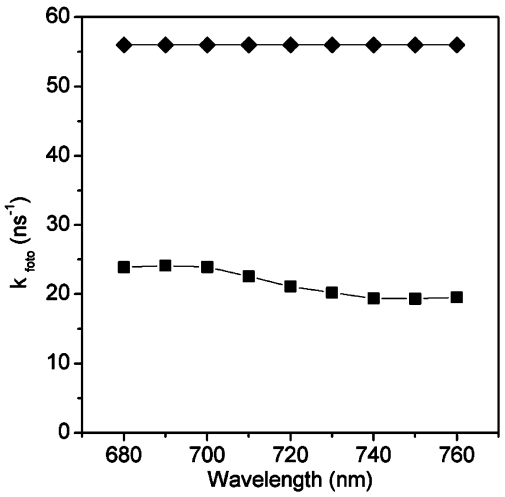

FIGURE 8: Mean values for the effective photosystem rate of primary photochemistry, $(\tau_{CS}^{eff})^{-1}$, of PSI−LHCI (squares) and of the PSI core (diamonds).

emission. This is the point of view taken in the compartmental modeling discussed below.

The following part of this study is aimed at a better understanding of the hitherto unexplained presence of two distinct slow fluorescence decays with only positive amplitudes, i.e., pure trapping components. This problem is addressed by simple compartmental modeling of the multicomponent fluorescence decay in which the number of experimental parameters (decay components) resembles the number of model states (compartments). This is not the case in the structure-based modeling studies which have emerged in recent years. Furthermore, as pointed out by Gobets et al. (*17*) this kind of modeling permits attention to be focused on some particular photosystem property which need not come out at all clearly in the complexity of modeling with 100−200 model states, of experimentally undefined energy and transition dipole orientation. In the present case, this particular photosystem property is the all-positive amplitudes of the two pure trapping components of PSI−LHCI.

The minimal compartment model should include just three compartmental states (bulk antenna, F735, F713), connected by reversible first-order rate processes. This is a number of compartments comparable with previous models of this kind for PSI (*17*, *31*). These are shown in Figure 7A. Trapping is modeled as occurring from the bulk pigments and is represented by a single rate process (k_{cs}). The details of PSI trapping, actively discussed in the literature at the present moment (*14*, *15*, *32*, *33*), are all summarized in this process (k_{cs}), which may be either reversible or irreversible. Here it is, simply, the effective trapping rate of the photosystem in the absence of the red forms F735 and F713. It will be immediately obvious that this minimal model, like all previous models in the literature, yields only one pure trapping component with all positive amplitudes, which, of course, is the slowest decay. Thus the minimal model is not qualitatively in agreement with experimental data on PSI−LHCI, and further detail is required. We have sought this detail in terms of antenna processes because, as discussed above, from the data on the PSI core, it seems to be the antenna which generates the biexponential trapping decay. This search was focused on the two low-energy spectral emission forms, F713 and F735, of LHCI as it was shown (Figure 6) that the ≈30 and ≈79 ps DAS are due to different ratios of these forms. Furthermore, our earlier analysis of the PSI fluorescence decay (*10*) indicated that the thermal activation energy for excited state trapping increased with increasing wavelength and was greatest for that region of the emission spectrum dominated by F735. This indicates that the slowest energy transfer processes are associated with this form. In this context, it is interesting that the F735 form seems to be present in two copies in each PSI−LHCI, as in vitro reconstitution experiments with recombinant Lhca1−4 apoproteins indicate that it is bound to both Lhca3 and Lhca4 (*28*). It is therefore not unreasonable to think that energy transfer from the bulk chlorophylls, most of which are in the core, may not be equal for the two copies of this low-energy state. We therefore hypothesize that transfer into and out of the F735 chlorophyll states is kinetically heterogeneous and rate limiting for trapping. This suggestion is shown in the compartment diagram of Figure 7B in which the three antenna energy levels explicitly present are associated with four model compartments. No attempt is made in this model to describe core or even LHCI processes. Its aim is exclusively to demonstrate that the idea of kinetic heterogeneity for transfer to the same spectral form can explain why the ≈30 and ≈79 ps trapping decays have only positive amplitudes. With this model, solutions can easily be found in which the decay is characterized by two pure trapping DAS components, both with all-positive amplitudes. It is also not difficult to find model solutions which bear a close resemblance to the ≈30 and ≈79 ps DAS band shapes and amplitudes of Figure 2 and which when taken together account for 90% of excited state trapping. An example of this is given by the rate constant numbers given in Figure 8, the results of which are presented in Table 1. This is not to be understood as a detailed compartmental model description due to the above-discussed broadness of the fit minimum. It is presented simply as an example on the basis of which we conclude that the hypothesis of heterogeneous transfer rates

Table 1: Fluorescence Decay Results of Compartmental Model Calculations of Figure 8B for Two Long-Wavelength Fluorescence Forms, F735 and F713[a]

	lifetime	
antenna state	31 ps	80 ps
F713	7.9 (0.3)	1.6 (0.09)
F735	18.6 (0.7)	15.8 (0.91)

[a] The numbers are the relative amplitudes of the two antenna states for each of the two decay components. The relative amplitudes, normalized to 1, for each of the two components are given in parentheses.

to the F735 low-energy fluorescence state provides a feasible explanation for the two all-positive DAS components in PSI−LHCI, without invoking reversible reaction center processes. In the model the indicative rate number ratios presented, by way of an example, are the population-weighted Boltzmann factors for the bulk−F735 transfers, while they come from the fit for the bulk−F713 transfer as we do not know the stoichiometry of this red chl form. The rate values themselves are fit parameters.

We now address the question of the effect of the external antenna on the effective photosystem photochemical trapping rate [$(\tau_{cs}^{eff})^{-1}$] in PSI−LHCI. As previously discussed (*10*) the value of this parameter is not constant over the 680−770 nm measurement wavelength range but decreases from about 24 ns^{-1} in the bulk emission region to about 19 ns^{-1} above 740 nm (Figure 8). These values are derived from the two pure trapping decays of 30 and 79 ps, which account for at least 90% of trapped excited states. On the other hand, the PSI core appears to have a single trapping component (17 ± 5 ps), which yields a $(\tau_{cs}^{eff})^{-1}$ value of 59 ± 13 ns^{-1} and which obviously is constant at all wavelengths (Figure 8). It is therefore evident that the external antenna has a marked "slowing down" influence on $(\tau_{cs}^{eff})^{-1}$, the extent of which is somewhat wavelength dependent. For the bulk antenna region the core/PSI−LHCI ratio is 2.5 and increases to 3.1 in the red. This is a large antenna effect if one only considers the relatively small change in antenna dimensions, about 95 chlorophylls for the core and 160 for the core plus outer antenna (PSI−LHCI). In the case of PSII we found an core/core *plus* outer antenna photochemical rate ratio of approximately 3.3 for $(\tau_{cs}^{eff})^{-1}$ (*18*), but in that case the antenna dimension increase (degeneracy) is at least a 5-fold one. Thus the outer antenna of PSI slows down the value of $(\tau_{cs}^{eff})^{-1}$ by almost the same amount as in PSII even though the increase in antenna degeneracy is much smaller. The reason for this is presumably due to the presence of quite high levels of low-energy chlorophyll forms in LHCI, while the outer antenna complexes of PSII are almost isoenergetic with the core. This pronounced slowing down effect of the red forms has often been predicted on the basis of model calculations (e.g., refs *31*, *34*, and *35*) due to the thermally activated energy transfer from the red forms toward the reaction center (*10*). Here this aspect is experimentally demonstrated for the first time.

Unfortunately on the basis of the present data, it is not possible to exactly quantify this "red form" effect as it is mixed in with the antenna size (degeneracy) effect. However, if we assume, as most theoretical considerations suggest, that the antenna size effect scales linearly with the degeneracy, we may expect that the degeneracy will slow down $(\tau_{cs}^{eff})^{-1}$ by a factor of about 95/160. This would decrease $(\tau_{cs}^{eff})^{-1}$ from the "core" mean value of $\approx$59 ns^{-1} to 35 ns^{-1}, a decrease of 0.41. The experimental mean values for PSI−LHCI vary from 24 ns^{-1} at 680 nm to 19 ns^{-1} at 740 nm. As the low-energy states are more heavily populated than the bulk, with approximately 80% of the excited states being associated with them in the steady state, the mean value over the 680−760 nm interval comes out near 20 ns^{-1}. Thus we conclude that the F735 and F713 antenna forms in LHCI slow down the effective photosystem rate of primary photochemistry by a factor of about $15/35 = 0.43$. This decrease is therefore approximately equal to that induced by the antenna size (degeneracy).

REFERENCES

1. Bruce, B. D., and Malkin, R. (1988) Subunit stoichiometry of the chloroplast photosystem I complex, *J. Biol. Chem. 263*, 7302−7308.
2. Ben-Shem, A., Frolow, F., and Nelson, N. (2003) Crystal structure of plant photosystem I, *Nature 426*, 630−635.
3. Jordan, P., Fromme, P., Witt, H. T., Klukas, O., Saenger, W., and Krauss, N. (2001) Three-dimensional structure of cyanobacterial photosystem I at 2.5 angstrom resolution, *Nature 411*, 909−917.
4. Jennings, R. C., Bassi, R., and Zucchelli, G. (1996) Antenna structure and energy transfer in higher plants photosystems, *Top. Curr. Chem. 177*, 147−181.
5. Boekema, E. J., Jensen, P. E., Schlodder, E., van Breemen, J. F. L., van Roon, H., Scheller, H. V., and Dekker, J. P. (2001) Green plant photosystem I binds light-harvesting complex I on one side of the complex, *Biochemistry 40*, 1029−1036.
6. Croce, R., and Bassi, R. (1998) The light-harvesting complex of photosystem I: pigment composition and stoichiometry, in *Photosyntesis: Mechanisms and Effects* (Garab, G., Ed.) Vol. 1, pp 421−424, Kluwer Academic Publishers, Dordrecht.
7. Croce, R., Zucchelli, G., Garlaschi, F. M., Bassi, R., and Jennings, R. C. (1996) Excited-state equilibration in the photosystem I light-harvesting I complex: P700 is almost isoenergetic with its antenna, *Biochemistry 35*, 8572−8579.
8. Croce, R., Zucchelli, G., Garlaschi, F. M., and Jennings, R. C. (1998) A thermal broadening study of the antenna chlorophylls in PSI-200, LHCI, and PSI core, *Biochemistry 37*, 17355−17360.
9. Croce, R., Dorra, D., Holzwarth, A. R., and Jennings, R. C. (2000) Fluorescence decay and spectral evolution in intact photosystem I of higher plants, *Biochemistry 39*, 6341−6348.
10. Jennings, R. C., Zucchelli, G., Croce, R., and Garlaschi, F. M. (2003) The photochemical trapping rate from red spectral states in PSI-LHCI is determined by thermal activation of energy transfer to bulk chlorophylls, *Biochim. Biophys. Acta 1557*, 91−98.
11. Byrdin, M., Rimke, I., Schlodder, E., Stehlik, D., and Roelofs, T. A. (2000) Decay kinetics and quantum yields of fluorescence in photosystem I from *Synechococcus elongatus* with P700 in the reduced and oxidized state: are the kinetics of excited-state decay trap-limited or transfer-limited?, *Biophys. J. 79*, 992−1007.
12. Turconi, S., Kruip, J., Schweitzer, G., Rogner, M., and Holzwarth, A. R. (1996) A comparative fluorescence kinetics study of photosystem I monomers and trimers from *Synechocystis* pcc 6803, *Photosynth. Res. 49*, 263−268.
13. Ihalainen, J. A., Jensen, P. E., Haldrup, A., van Stokkum, I. H. M., van Grondelle, R., Scheller, H. V., and Dekker, J. P. (2002) Pigment organization and energy transfer dynamics in isolated, photosystem I (PSI) complexes from *Arabidopsis thaliana* depleted of the PSI-G, PSI-K, PSI-L, or PSI-N subunit, *Biophys. J. 83*, 2190−2201.
14. Muller, M. G., Niklas, J., Lubitz, W., and Holzwarth, A. R. (2003) Ultrafast transient absorption studies on photosystem I reaction centers from *Chlamydomonas reinhardtii*. 1. A new interpretation of the energy trapping and early electron-transfer steps in photosystem I, *Biophys. J. 85*, 3899−3922.
15. Holzwarth, A. R., Muller, M. G., Niklas, J., and Lubitz, W. (2005) Charge recombination fluorescence in photosystem I reaction centers from *Chlanydomonas reinhardtii*, *J. Phys. Chem. B 109*, 5903−5911.

16. Hastings, G., Kleinherenbrink, F. A. M., Lin, S., and Blankenship, R. E. (1994) Time-resolved fluorescence and absorption-spectroscopy of photosystem I, *Biochemistry 33*, 3185−3192.
17. Gobets, B., van Stokkum, I. H. M., Rogner, M., Kruip, J., Schlodder, E., Karapetyan, N. V., Dekker, J. P., and van Grondelle, R. (2001) Time-resolved fluorescence emission measurements of photosystem I particles of various cyanobacteria: A unified compartmental model, *Biophys. J. 81*, 407−424.
18. Engelmann, E. C. M., Zucchelli, G., Garlaschi, F. M., Casazza, A. P., and Jennings, R. C. (2005) The effect of outer antenna complexes on the photochemical trapping rate in barley thylakoid photosystem II, *Biochim. Biophys. Acta 1706*, 276−286.
19. Jennings, R. C., Bassi, R., Garlaschi, F. M., Dainese, P., and Zucchelli, G. (1993) Distribution of the chlorophyll spectral forms in the chlorophyll-protein complexes of photosystem II antenna, *Biochemistry 32*, 3203−3210.
20. Jennings, R. C., Garlaschi, F. M., Bassi, R., Zucchelli, G., Vianelli, A., and Dainese, P. (1993) A study of photosystem-II fluorescence emission in terms of the antenna chlorophyll-protein complexes, *Biochim. Biophys. Acta 1183*, 194−200.
21. Laemmli, U. K. (1970) Cleavage of structural proteins during the assembly of the head of bacteriophage T4, *Nature 227*, 680−685.
22. Carbonera, D., Collareta, P., and Giacometti, G. (1997) *Biochim. Biophys. Acta 1322*, 115−128.
23. Santabarbara, S., Bordignon, E., Jennings, R. C., Carbonera, D. (2002) Chlorophyll triplet states associated with photosytem II of thylakoids, *Biochemistry 41*, 8184−8194.
24. Ihalainen, J. A., van Stokkum, I. H. M., Gibasiewicz, K., Germano, M., van Grondelle, R., and Dekker, J. P. (2005) Kinetics of excitation trapping in intact photosystem I of *Chlamydomonas reinhardtii* and *Arabidopsis thaliana*, *Biochim. Biophys. Acta 1706*, 267−275.
25. Trinkunas, G., and Holzwarth, A. R. (1994) Kinetic modeling of exciton migration in photosynthetic systems. 2. Simulations of excitation dynamics in 2-dimensional photosystem core antenna/reaction center complexes, *Biophys. J. 66*, 415−429.
26. Trinkunas, G., and Holzwarth, A. R. (1996) Kinetic modeling of exciton migration in photosynthetic systems. 3. Application of genetic algorithms to simulations of excitation dynamics in three-dimensional photosystem core antenna reaction center complexes, *Biophys. J. 71*, 351−364.
27. Ihalainen, J. A., Gobets, B., Sznee, K., Brazzoli, M., Croce, R., Bassi, R., van Grondelle, R., Korppi-Tommola, J. E. I., and Dekker, J. P. (2000) Evidence for two spectroscopically different dimers of light-harvesting complex I from green plants, *Biochemistry 39*, 8625−8631.
28. Morosinotto, T., Breton, J., Bassi, R., and Croce, R. (2003) The nature of a chlorophyll ligand in Lhca proteins determines the far red fluorescence emission typical of photosystem I, *J. Biol. Chem. 278*, 49223−49229.
29. Jennings, R. C., Zucchelli, G., Engelmann, E., and Garlaschi, F. M. (2004) The long-wavelength chlorophyll states of plant LHCI at room temperature: a comparison with PSI-LHCI, *Biophys. J. 87*, 488−497.
30. Zucchelli, G., Morosinotto, T., Garlaschi, F. M., Bassi, R., and Jennings, R. C. (2005) The low energy emitting states of the Lhca4 subunit of higher plant photosystem I, *FEBS Lett. 579*, 2071−2076.
31. Jennings, R. C., Zucchelli, G., Croce, R., Valkunas, L., Finzi, L., and Garlaschi, F. M. (1997) Model studies on the excited-state equilibrium perturbation due to reaction centre trapping in photosystem I, *Photosynth. Res. 52*, 245−253.
32. Santabarbara, S., Heathcote, P., and Evans, M. C. W. (2005) Modelling of the electron-transfer reactions in photosystem I by electron tunnelling theory: the phylloquinones bound to the PsaA and the PsaB reaction centre subunits of PSI are almost isoenergetic to the iron-sulfur cluster Fx, *Biochim. Biophys. Acta 1708*, 283−310.
33. Gobets, B., and van Grondelle, R. (2001) Energy transfer and trapping in photosystem I, *Biochim. Biophys. Acta 1507*, 80−99.
34. Fischer, M. R., and Hoff, A. J. (1992) On the long-wavelength component of the light-harvesting complex of some photosynthetic bacteria, *Biophys. J. 63*, 911−916.
35. Trissl, H. W. (1993) Long-wavelength absorbing antenna pigments and heterogeneous absorption bands concentrate excitons and increase absorption cross section, *Photosynth. Res. 35*, 247−263.

BI060243P